

GENERALIZED FRACTIONAL BÉZIER-LIKE CURVE AND SURFACE WITH APPLICATIONS

**SYED AHMAD AIDIL ADHA
BIN SAID MAD ZAIN**

UNIVERSITI SAINS MALAYSIA

2024

GENERALIZED FRACTIONAL BÉZIER-LIKE CURVE AND SURFACE WITH APPLICATIONS

by

**SYED AHMAD AIDIL ADHA
BIN SAID MAD ZAIN**

**Thesis submitted in fulfilment of the requirements
for the degree of
Doctor of Philosophy**

August 2024

ACKNOWLEDGEMENT

Alhamdulillah, praise to Allah S.W.T and peace be upon His beloved prophet Muhammad S.A.W for allowing me to complete this thesis. Despite the COVID-19 pandemic virus that poses threat to humanity from the year 2020 to 2022, the guide from Allah S.W.T and the unwavering support from my family, friends and university contribute to my journey of completing this thesis. I would like to express my sincere gratitude to my supervisor, Dr. Md Yushalify Misro, for his invaluable advice and guidance. Despite my limited research experience due to skipping Master's degree, he always supports and keep giving me advice, especially when I am at my lowest point. I also extend my heartfelt appreciation to Prof. Dr. Kenjiro T. Miura from Shizuoka University, Japan, for his invaluable advisory role in the journal publications. My deepest gratitude to both of them for becoming the pillars of my Ph.D. journey. Not to forget my queen and king of my heart, my mother, Fadzilah Sudin, and my father, Said Mad Zain Said Akil, who gave non-stop motivation and support throughout thick and thin. A special gratitude to the love of my life, my wife, Noraini Zulkifli, for the emotional support and unwavering presence since the day we married. I also want to thank my friends in the School of Mathematical Sciences and the Student Representative Council at USM for accompanying me on my journey. I am truly thankful to Allah for blessing me with such wonderful parents, supportive wife, and incredible friends. Lastly, I sincerely thank GRA-Assist USM for the financial support during my first year, GREP-MARA during my second year, and MyBrainSc from the Ministry of Higher Education during my third year. It is with their support that I have been able to complete this thesis.

TABLE OF CONTENTS

ACKNOWLEDGEMENT	ii
TABLE OF CONTENTS	iii
LIST OF TABLES	ix
LIST OF FIGURES	x
LIST OF ALGORITHMS	xxxiii
LIST OF ABBREVIATIONS	xxxiv
LIST OF SYMBOLS	xxxv
ABSTRAK	xxxvii
ABSTRACT	xxxviii
CHAPTER 1 INTRODUCTION	1
1.1 Introduction: History of CAGD and Origin of Fractional Calculus	1
1.2 Motivation	10
1.3 Problem Statements	12
1.4 Objectives	12
1.5 Scope and Limitations	13
1.6 Outline of Thesis	13
CHAPTER 2 BACKGROUND AND LITERATURE REVIEW	16
2.1 Parametric Curves and Surfaces	16
2.1.1 Bézier Curves and Surfaces	17
2.1.2 Aesthetic Bézier Curves and Surfaces	18
2.2 Fairness Metric of Construction of Smooth Curve and Surface	21
2.2.1 Continuity of The Curve	22
2.2.2 The Internal Energy of Curve	23

2.2.3	Curvature Analysis of Curves	24
2.2.3(a)	Curvature Plot	25
2.2.3(b)	Curvature Comb	26
2.2.4	Continuity of The Surface	27
2.2.5	The Internal Energy of Surface	28
2.2.6	Curvature Analysis of Surfaces.....	29
2.2.6(a)	Gaussian Curvature of Surface	30
2.2.6(b)	Mean Curvature of Surface	31
2.3	Curve Fitting	32
2.4	κ -Curve	33
2.5	Engineering Surfaces	35
2.6	Fractional Calculus: From Riemann-Liouville Definition to Present-Day Definition	36
2.7	Mathematical Harmony: Synergy between CAGD and Fractional Calculus .	39
CHAPTER 3	GENERALIZED FRACTIONAL BÉZIER-LIKE CURVE WITH SHAPE PARAMETERS	42
3.1	Introduction	42
3.2	Generalized Fractional Bézier-Like Function	42
3.2.1	Riemann–Liouville Fractional Integral	42
3.2.2	Generalized Fractional Bézier-Like Function Definition.....	43
3.2.3	Properties of Generalized Fractional Bézier-Like Functions	44
3.3	Generalized Fractional Bézier-Like Curve with Shape Parameters	52
3.3.1	Properties of Generalized Fractional Bézier-Like Curve.....	53
3.3.2	Properties of Curve	53
3.4	The Impact of Shape and Fractional Parameters on Geometric Behaviour of Curve.....	57

3.4.1	The Significance of Shape Parameters on Geometric Behaviour of Curve	57
3.4.2	The Significance of Fractional Parameters on Geometric Behaviour of Curve	60
3.5	Fractional De Casteljau Algorithm for Curve Construction	61
3.6	Designing of Shapes from Generalized Fractional Bézier-Like Curves	63
3.7	Curvature Analysis of Generalized Fractional Bézier-Like Curve	66
3.8	Fairness Metric of Generalized Fractional Bézier-Like Curve using Internal Energy	68
3.8.1	Fractional Parameters Influence on The Internal Energy of Curve ...	70
3.8.2	Shape Parameters Influence on The Internal Energy of Curve.....	73
3.9	Summary	75
CHAPTER 4	GENERALIZED FRACTIONAL BÉZIER-LIKE SURFACE WITH SHAPE PARAMETERS	76
4.1	Introduction	76
4.2	Generalized Fractional Bézier-Like Tensor Product Surface	76
4.2.1	Properties of Generalized Fractional Bézier-Like Tensor Product Surface	77
4.3	Geometric Impact of Shape and Fractional Parameters on The Surface	78
4.3.1	Shape Parameters Impact on Geometric Behaviour of Surface	78
4.3.2	Fractional Parameters Impact on Geometric Behaviour of Surface ..	84
4.4	Fractional De Casteljau Algorithm for Surface Construction	87
4.5	Modelling of Simple Surfaces using Generalized Fractional Bézier-Like Surface	91
4.5.1	Surface Revolution	91
4.5.2	Extruded Surface	94
4.6	Curvature Analysis of Generalized Fractional Bézier-Like Surface	95

4.6.1	Categorization of Surface Points Via Gaussian and Mean Curvatures	98
4.6.2	Example of Surface Analysis for Generalized Fractional Bézier-Like Surface	101
4.6.2(a)	The Role of Fractional Parameter in Surface Analysis	101
4.6.2(b)	The Role of Shape Parameter in Surface Analysis	107
4.7	Fairness Metric of Generalized Fractional Bézier-Like Surface using Internal Energy	110
4.7.1	Fractional Parameters Influence on The Internal Energy of Surface ..	111
4.7.2	Shape Parameters Influence on The Internal Energy of Surface	118
4.8	Summary	120
CHAPTER 5 CONTINUITY CONDITIONS FOR GENERALIZED FRACTIONAL BÉZIER-LIKE CURVES		122
5.1	Introduction	122
5.2	Continuity Conditions for Generalized Fractional Bézier-Like Curves.....	123
5.2.1	C^r Continuity for Generalized Fractional Bézier-Like Curves.....	123
5.2.2	G^r Continuity for Generalized Fractional Bézier-Like Curves	129
5.2.3	F^r Continuity for Generalized Fractional Bézier-Like Curves	135
5.3	Fairness Metric of Piecewise Generalized Fractional Bézier-Like Curves Using Curvature Plot and Comb	150
5.3.1	Fairness Metric in Behaviour of Curvature Plot and Comb of Parametric Continuity.....	154
5.3.2	Fairness Metric in Behaviour of Curvature Plot and Comb of Geometric Continuity	157
5.3.3	Fairness Metric in Behaviour of Curvature Plot and Comb of Fractional Continuity	159
5.4	Summary	162
CHAPTER 6 CONTINUITY CONDITIONS FOR GENERALIZED FRACTIONAL BÉZIER-LIKE SURFACES		163

6.1	Introduction	163
6.2	Fractional Continuity Conditions for Generalized Fractional Bézier-Like Surfaces	163
6.2.1	s Direction F^2 Continuity	167
6.2.2	s and t Directions F^2 Continuity	175
6.2.3	t Direction F^2 Continuity	180
6.3	Procedures and Example of Fractional Continuity for Generalized Fractional Bézier-Like Surfaces	181
6.3.1	Procedures: Fractional Continuity for Generalized Fractional Bézier-Like Surfaces	181
6.3.2	Examples: Generalized Fractional Bézier-Like Surfaces with F^2 Continuity	182
6.3.2(a)	Fractional Parameters Impact on The Fractional Continuity	182
6.3.2(b)	Shape Parameters Impact on The Fractional Continuity ...	186
6.3.2(c)	Scale Factor Impact on The Fractional Continuity	188
6.3.3	F^2 Continuity of Three Consecutive Fractional Bézier-Like Surfaces	189
6.4	The Behaviour of Gaussian and Mean Curvatures in F^2 Continuity	190
6.5	Summary	195
CHAPTER 7 APPLICATIONS OF GENERALIZED FRACTIONAL BÉZIER-LIKE CURVE AND SURFACE		197
7.1	Introduction	197
7.2	Curve Fitting using Generalized Fractional Bézier-Like Curve	197
7.2.1	Application of Fractional Parameters in Curve Fitting	198
7.2.2	Curve Fitting Process	199
7.3	Construction of κ -Curve Using Generalized Fractional Bézier-Like Curve ..	211
7.3.1	Formulation of κ -Curve using Generalized Fractional Bézier-Like Curve	211

7.3.2	Algorithm for Construction of Piecewise Open κ -Curve using Fractional Bézier-Like Curve	215
7.3.3	Algorithm for Construction of Piecewise Closed κ -Curve using Fractional Bézier-Like Curve	217
7.3.4	Comparison Between Fractional Bézier-Like Curve and κ -Curve ...	223
7.4	Modelling of Engineering Surfaces using Generalized Fractional Bézier-Like Surface	225
7.4.1	Construction of Generalized Fractional Bézier-Like Ruled Surface ..	225
7.4.2	Construction of Generalized Fractional Bézier-Like Swept Surface .	233
7.4.3	Construction of Generalized Fractional Bézier-Like Swung Surface	238
7.4.4	Construction of Generalized Fractional Bézier-Like Rotation Surface	244
7.5	Summary	248
CHAPTER 8 CONCLUSION		250
8.1	Introduction	250
8.2	Research Conclusion	250
8.3	Future Work and Recommendations	253
REFERENCES		255
APPENDICES		
LIST OF PUBLICATIONS		

LIST OF TABLES

		Page
Table 3.1	Stretch energy, bending energy, and curvature variation energy for cubic fractional Bézier-like curve with different shape parameters and fractional parameter. Fractional parameter with * are the critical values.	72
Table 3.2	Stretch energy, bending energy, and curvature variation energy for cubic fractional Bézier-like curve with different shape parameters but zero values of fractional parameters.	74
Table 4.1	Categorization of local geometry point of surface by inspection of Gaussian, mean and principal curvatures.	98
Table 4.2	Categorization of type of surfaces according to Gaussian and mean curvatures signs.	98
Table 4.3	Stretch energy and bending energy for bicubic fractional Bézier-like surface with different values of fractional parameters.	115
Table 4.4	Stretch and bending energies via manipulation of shape parameters for bicubic fractional Bézier-like surface.	118
Table 6.1	Gaussian and mean curvatures value according to the respective value of shape parameters and free parameter, s .	192
Table 6.2	Gaussian and mean curvatures value according to the respective value of fractional parameters, $v_{1,2}$ and free parameter, s .	194
Table 7.1	Comparison between κ -curves, $\varepsilon\kappa$ -curves and fractional Bézier-like curves.	224
Table 8.1	The comparison between several aesthetic Bézier-like representation with generalized fractional Bézier-like representation.	253

LIST OF FIGURES

	Page
Figure 2.1 Classical cubic Bézier curves with different set of control	18
points.	
Figure 2.1(a) First set of control points.	18
Figure 2.1(b) Second set of control points.	18
Figure 2.2 Classical cubic Bézier curves with its curvature plot.	25
Figure 2.2(a) Classical cubic Bézier curve.	25
Figure 2.2(b) The curvature plot of curve in (a).	25
Figure 2.3 Classical cubic Bézier curve with its curvature comb.	27
Figure 3.1 Fractional Bézier-like functions of quadratic degree with.....	51
varying shape and fractional parameters	
Figure 3.1(a) $v = 0$	51
Figure 3.1(b) $v = 0.5$	51
Figure 3.1(c) $v = 0.75$	51
Figure 3.1(d) $v = 1.25$	51
Figure 3.2 Fractional Bézier-like functions of cubic degree with varying.....	51
shape and fractional parameters.	
Figure 3.2(a) $v = 0$	51
Figure 3.2(b) $v = 0.5$	51
Figure 3.2(c) $v = 1$	51
Figure 3.3 Cubic fractional Bézier-like curve with varying shape pa-	59
rameters with $v = 0$.	
Figure 3.3(a) $t = 0.25$	59
Figure 3.3(b) $t = 0.5$	59

Figure 3.3(c)	$t = 0.75$.	59
Figure 3.4	Cubic fractional Bézier-like curve with varying fractional parameters.	61
Figure 3.4(a)	$\nu = 0$.	61
Figure 3.4(b)	$\nu = 0.5$.	61
Figure 3.4(c)	$\nu = 1$.	61
Figure 3.5	Fractional De Casteljau Algorithm Triangle Scheme.	63
Figure 3.6	Modelling shape of heart with different shape and fractional parameters.	64
Figure 3.6(a)	$\nu = 0$.	64
Figure 3.6(b)	$\nu = 0.5$.	64
Figure 3.6(c)	$\nu = 1$.	64
Figure 3.7	Modelling shape of petal with different shape and fractional parameters.	64
Figure 3.7(a)	$\nu = 0$.	64
Figure 3.7(b)	$\nu = 0.5$.	64
Figure 3.7(c)	$\nu = 1$.	64
Figure 3.8	Modelling shape of flower with different values of fractional parameters.	65
Figure 3.8(a)	$\nu_i = 0$.	65
Figure 3.8(b)	$\nu_1 = \nu_2 = 2.1$.	65
Figure 3.8(c)	$\nu_1 = \nu_2 = 2.1, \nu_5 = 0.31, \nu_7 = 1, \nu_{10} = 1.2$.	65
Figure 3.8(d)	$\nu_5 = 1.04, \nu_7 = 2.18, \nu_8 = 1.25, \nu_{10} = 1.85$.	65
Figure 3.9	Cubic fractional Bézier-like curve with its curvature plot and curvature comb.	68
Figure 3.9(a)	$\nu = 0$.	68
Figure 3.9(b)	$\nu = 0.5$.	68

Figure 3.9(c)	$\nu = 0.75$.	68
Figure 3.10	Multiple curves of cubic fractional Bézier-like with different shape and fractional parameters and their respective curvature plots.	71
Figure 3.10(a)	$\nu = 0.5$.	71
Figure 3.10(b)	$\nu = 0.8$.	71
Figure 3.10(c)	$\nu = 2$.	71
Figure 3.10(d)	Curvature plot $\nu = 0.5$.	71
Figure 3.10(e)	Curvature plot $\nu = 0.8$.	71
Figure 3.10(f)	Curvature plot $\nu = 2$.	71
Figure 3.11	Multiple curves of cubic fractional Bézier-like with different shape and fractional parameters with their respective curvature plots.	73
Figure 3.11(a)	Multiple a_1 values.	73
Figure 3.11(b)	Multiple a_2 values.	73
Figure 3.11(c)	Multiple a_3 values.	73
Figure 3.11(d)	Curvature plot with multiple a_1 values.	73
Figure 3.11(e)	Curvature plot with multiple a_2 values.	73
Figure 3.11(f)	Curvature plot with multiple a_3 values.	73
Figure 4.1	The mapping of shape parameters that are associated with their respective control points.	81
Figure 4.2	Process of minimizing the distance between biquartic fractional Bézier-like surface and $P_{2,2}$	83
Figure 4.2(a)	$(0, 0, 0, 0, 0, 0, 0, 0)$.	83
Figure 4.2(b)	$(0, 1.99, -1.99, 0, 0, 0, 0, 0)$.	83
Figure 4.2(c)	$(0, 1.99, -1.99, 0, 0, 1.99, -1.99, 0)$.	83
Figure 4.2(d)	$(0.99, 1.99, -1.99, -0.99, 0.99, 1.99, -1.99, -0.99)$.	83

Figure 4.3	Process of maximizing the distance between biquartic fractional Bézier-like surface and $P_{2,2}$.	84
Figure 4.3(a)	$(0, 0, 0, 0, 0, 0, 0, 0)$.	84
Figure 4.3(b)	$(0, -2.99, 2.99, 0, 0, 0, 0, 0)$.	84
Figure 4.3(c)	$(0, -2.99, 2.99, 0, 0, -2.99, 2.99, 0)$.	84
Figure 4.3(d)	$(-3.99, -2.99, 2.99, 3.99, -3.99, -2.99, 2.99, 3.99)$.	84
Figure 4.4	First variation of fractional parameters in biquartic fractional Bézier-like surface.	86
Figure 4.4(a)	$v_1 = 0.5$ and $v_2 = 0$.	86
Figure 4.4(b)	$v_1 = 0.5$ and $v_2 = 0.5$.	86
Figure 4.4(c)	$v_1 = 0.65$ and $v_2 = 0.5$.	86
Figure 4.4(d)	$v_1 = 0.65$ and $v_2 = 0.75$.	86
Figure 4.5	Second variation of fractional parameters in biquartic fractional Bézier-like surface.	87
Figure 4.5(a)	$v_1 = 0.5$ and $v_2 = 0$.	87
Figure 4.5(b)	$v_1 = 0.5$ and $v_2 = 0.5$.	87
Figure 4.5(c)	$v_1 = 0.65$ and $v_2 = 0.5$.	87
Figure 4.5(d)	$v_1 = 0.65$ and $v_2 = 0.75$.	87
Figure 4.6	Surface revolution of two consecutive cubic fractional Bézier-like curves with varying fractional parameters.	93
Figure 4.6(a)	$v_1 = 0.5$ and $v_2 = 0.75$.	93
Figure 4.6(b)	$v_1 = v_2 = 1$.	93
Figure 4.6(c)	$v_1 = 1.5$ and $v_2 = 2$.	93
Figure 4.6(d)	$v_1 = v_2 = 2.5$.	93
Figure 4.7	Surface revolution of two consecutive cubic fractional Bézier-like curves with varying shape parameters and fractional parameters.	93

Figure 4.7(a)	$v_1 = 0.5$ and $v_2 = 0.75$.	93
Figure 4.7(b)	$v_1 = v_2 = 1$.	93
Figure 4.7(c)	$v_1 = 1.5$ and $v_2 = 2$.	93
Figure 4.7(d)	$v_1 = v_2 = 2.5$.	93
Figure 4.8	Extruded surface from cubic fractional Bézier-like curves with various value of fractional parameter.	94
Figure 4.8(a)	$v = 0.5$.	94
Figure 4.8(b)	$v = 1$.	94
Figure 4.8(c)	$v = 2$.	94
Figure 4.9	Extruded surface from cubic fractional Bézier-like curves with various v .	95
Figure 4.9(a)	$v = 0.5$.	95
Figure 4.9(b)	$v = 1$.	95
Figure 4.9(c)	$v = 2$.	95
Figure 4.10	Torus with 3 types of different surface point such as elliptic, hyperbolic and parabolic point together with respective Gaussian and mean curvature.	99
Figure 4.10(a)	Gaussian curvature of torus.	99
Figure 4.10(b)	Mean curvature of torus.	99
Figure 4.11	Monkey saddle contained a planar point at the origin with zero values Gaussian and mean curvatures.	100
Figure 4.11(a)	Gaussian curvature of monkey saddle.	100
Figure 4.11(b)	Mean curvature of monkey saddle.	100
Figure 4.12	The behaviour of Gaussian and mean curvatures of bicubic Bézier surface via manipulation of fractional parameters.	102
Figure 4.12(a)	Gaussian: $v_1 = v_2 = 0$.	102
Figure 4.12(b)	Mean: $v_1 = v_2 = 0$.	102

Figure 4.12(c)	Gaussian: $v_1 = 0.6$ and $v_2 = 0$.	102
Figure 4.12(d)	Mean: $v_1 = 0.6$ and $v_2 = 0$.	102
Figure 4.12	(Continue 1) The behaviour of Gaussian and mean curvatures of bicubic Bézier surface via manipulation of fractional parameters.	103
Figure 4.12(e)	Gaussian: $v_1 = 1$ and $v_2 = 0$.	103
Figure 4.12(f)	Mean: $v_1 = 1$ and $v_2 = 0$.	103
Figure 4.12(g)	Gaussian: $v_1 = 0$ and $v_2 = 0.6$.	103
Figure 4.12(h)	Mean: $v_1 = 0$ and $v_2 = 0.6$.	103
Figure 4.12(i)	Gaussian: $v_1 = 0$ and $v_2 = 1$.	103
Figure 4.12(j)	Mean: $v_1 = 0$ and $v_2 = 1$.	103
Figure 4.12(k)	Gaussian: $v_1 = v_2 = 0.6$.	103
Figure 4.12(l)	Mean: $v_1 = v_2 = 0.6$.	103
Figure 4.12	(Continue 2) The behaviour of Gaussian and mean curvatures of bicubic Bézier surface via manipulation of fractional parameters.	104
Figure 4.12(m)	Gaussian: $v_1 = v_2 = 1$.	104
Figure 4.12(n)	Mean: $v_1 = v_2 = 1$.	104
Figure 4.13	The behaviour of Gaussian and mean curvatures of bicubic Bézier surface via manipulation of fractional parameters with different shape parameters.	104
Figure 4.13(a)	Gaussian: $v_1 = v_2 = 0$.	104
Figure 4.13(b)	Mean: $v_1 = v_2 = 0$.	104
Figure 4.13(c)	Gaussian: $v_1 = 0.6$ and $v_2 = 0$.	104
Figure 4.13(d)	Mean: $v_1 = 0.6$ and $v_2 = 0$.	104
Figure 4.13	(Continue 1) The behaviour of Gaussian and mean curvatures of bicubic Bézier surface via manipulation of fractional parameters with different shape parameters.	105

Figure 4.13(e)	Gaussian: $v_1 = 1$ and $v_2 = 0$.	105
Figure 4.13(f)	Mean: $v_1 = 1$ and $v_2 = 0$.	105
Figure 4.13(g)	Gaussian: $v_1 = 0$ and $v_2 = 0.6$.	105
Figure 4.13(h)	Mean: $v_1 = 0$ and $v_2 = 0.6$.	105
Figure 4.13(i)	Gaussian: $v_1 = 0$ and $v_2 = 1$.	105
Figure 4.13(j)	Mean: $v_1 = 0$ and $v_2 = 1$.	105
Figure 4.13(k)	Gaussian: $v_1 = v_2 = 0.6$.	105
Figure 4.13(l)	Mean: $v_1 = v_2 = 0.6$.	105
Figure 4.13	(Continue 2) The behaviour of Gaussian and mean curvatures of bicubic Bézier surface via manipulation of fractional parameters with different shape parameters.	106
Figure 4.13(m)	Gaussian: $v_1 = v_2 = 1$.	106
Figure 4.13(n)	Mean: $v_1 = v_2 = 1$.	106
Figure 4.14	The behaviour of Gaussian and mean curvatures of bicubic Bézier surface via manipulation of shape parameters.	107
Figure 4.14(a)	Gaussian: Shape parameters are $(0, 0, 0, 0, 0, 0)$.	107
Figure 4.14(b)	Mean: Shape parameters are $(0, 0, 0, 0, 0, 0)$.	107
Figure 4.14(c)	Gaussian: Shape parameters are $(0.99, 0, -0.99, 0.99, 0, -0.99)$.	107
Figure 4.14(d)	Mean: Shape parameters are $(0.99, 0, -0.99, 0.99, 0, -0.99)$.	107
Figure 4.14	(Continue 1) The behaviour of Gaussian and mean curvatures of bicubic Bézier surface via manipulation of shape parameters.	108
Figure 4.14(e)	Gaussian: Shape parameters are $(0.99, 1.99, -0.99, 0.99, 0, -0.99)$.	108
Figure 4.14(f)	Mean: Shape parameters are $(0.99, 1.99, -0.99, 0.99, 0, -0.99)$.	108

Figure 4.14(g)	Gaussian: Shape parameters are.....	108
	$(0.99, -1.99, -0.99, 0.99, 0, -0.99)$.	
Figure 4.14(h)	Mean: Shape parameters are.....	108
	$(0.99, -1.99, -0.99, 0.99, 0, -0.99)$.	
Figure 4.14(i)	Gaussian: Shape parameters are.....	108
	$(0.99, 0, -0.99, 0.99, 1.99, -0.99)$.	
Figure 4.14(j)	Mean: Shape parameters are.....	108
	$(0.99, 0, -0.99, 0.99, 1.99, -0.99)$.	
Figure 4.14	(Continue 2) The behaviour of Gaussian and mean curva-.....	109
	tures of bicubic Bézier surface via manipulation of shape pa- rameters.	
Figure 4.14(k)	Gaussian: Shape parameters are.....	109
	$(0.99, 0, -0.99, 0.99, -1.99, -0.99)$.	
Figure 4.14(l)	Mean: Shape parameters are.....	109
	$(0.99, 0, -0.99, 0.99, -1.99, -0.99)$.	
Figure 4.14(m)	Gaussian: Shape parameters are	109
	$(0.99, 1.99, -0.99, 0.99, 1.99, -0.99)$.	
Figure 4.14(n)	Mean: Shape parameters are	109
	$(0.99, 1.99, -0.99, 0.99, 1.99, -0.99)$.	
Figure 4.15	Multiple bicubic fractional Bézier-like surface with different.....	112
	values of fractional parameter and zero values of shape pa- rameters.	
Figure 4.15(a)	$v_1 = 0$ and $v_2 = 0$	112
Figure 4.15(b)	$v_1 = 0.6$ and $v_2 = 0$	112
Figure 4.15(c)	$v_1 = 1$ and $v_2 = 0$	112
Figure 4.15(d)	$v_1 = 0$ and $v_2 = 0.6$	112
Figure 4.15	(Continue) Multiple bicubic fractional Bézier-like surface	113
	with different values of fractional parameter and zero val- ues of shape parameters.	
Figure 4.15(e)	$v_1 = 0$ and $v_2 = 1$	113
Figure 4.15(f)	$v_1 = 0.6$ and $v_2 = 0.6$	113

Figure 4.15(g)	$v_1 = 1$ and $v_2 = 1$	113
Figure 4.16	Multiple bicubic fractional Bézier-like surface with different values of fractional parameter and $(-1.5, 0, 1.5, -1.5, 0, 1.5)$ shape parameters.	114
Figure 4.16(a)	$v_1 = 0$ and $v_2 = 0$	114
Figure 4.16(b)	$v_1 = 0.6$ and $v_2 = 0$	114
Figure 4.16(c)	$v_1 = 1$ and $v_2 = 0$	114
Figure 4.16(d)	$v_1 = 0$ and $v_2 = 0.6$	114
Figure 4.16(e)	$v_1 = 0$ and $v_2 = 1$	114
Figure 4.16(f)	$v_1 = 0.6$ and $v_2 = 0.6$	114
Figure 4.16	(Continue) Multiple bicubic fractional Bézier-like surface with different values of fractional parameter and $(-1.5, 0, 1.5, -1.5, 0, 1.5)$ shape parameters.	115
Figure 4.16(g)	$v_1 = 1$ and $v_2 = 1$	115
Figure 4.17	Gaussian and mean curvatures of some of the figures in Figure 4.15.	117
Figure 4.17(a)	Gaussian: $v_1 = 0.6$ and $v_2 = 0$	117
Figure 4.17(b)	Mean: $v_1 = 0.6$ and $v_2 = 0$	117
Figure 4.17(c)	Gaussian: $v_1 = 0$ and $v_2 = 0.6$	117
Figure 4.17(d)	Mean: $v_1 = 0$ and $v_2 = 0.6$	117
Figure 4.17(e)	Gaussian: $v_1 = 0.6$ and $v_2 = 0.6$	117
Figure 4.17(f)	Mean: $v_1 = 0.6$ and $v_2 = 0.6$	117
Figure 4.18	Gaussian and mean curvatures of bicubic fractional Bézier-like surface with various values of shape parameters.	119
Figure 4.18(a)	Gaussian: $(0, 0, 0, 0, 0, 0)$	119
Figure 4.18(b)	Mean: $(0, 0, 0, 0, 0, 0)$	119
Figure 4.18(c)	Gaussian: $(-2.9, 0, 2.9, -2.9, 0, 2.9)$	119

Figure 4.18(d) Mean: $(-2.9, 0, 2.9, -2.9, 0, 2.9)$	119
Figure 4.18(e) Gaussian: $(0.9, 0, -0.9, 0.9, 0, -0.9)$	119
Figure 4.18(f) Mean: $(0.9, 0, -0.9, 0.9, 0, -0.9)$	119
Figure 5.1 C^0 continuity of two cubic fractional Bézier-like curves.	127
Figure 5.1(a) $v_2 = 0.5$	127
Figure 5.1(b) $v_2 = 0.75$	127
Figure 5.1(c) $v_2 = 1$	127
Figure 5.1(d) $v_2 = 1.5$	127
Figure 5.2 C^1 continuity of two cubic fractional Bézier-like curves.	128
Figure 5.2(a) $v_2 = 0.5$	128
Figure 5.2(b) $v_2 = 0.75$	128
Figure 5.2(c) $v_2 = 1$	128
Figure 5.2(d) $v_2 = 1.5$	128
Figure 5.3 C^2 continuity of two cubic fractional Bézier-like curves.	128
Figure 5.3(a) $v_2 = 0.5$	128
Figure 5.3(b) $v_2 = 0.75$	128
Figure 5.3 (Continue) C^2 continuity of two cubic fractional Bézier-like	129
curves.	
Figure 5.3(c) $v_2 = 1$	129
Figure 5.3(d) $v_2 = 1.5$	129
Figure 5.4 G^1 continuity of two cubic fractional Bézier-like curves.	133
Figure 5.4(a) $v_2 = 0.5$	133
Figure 5.4(b) $v_2 = 0.75$	133
Figure 5.4(c) $v_2 = 1$	133
Figure 5.4(d) $v_2 = 1.5$	133

Figure 5.5	G^2 continuity of two cubic fractional Bézier-like curves.	134
Figure 5.5(a)	$v_2 = 0.5$	134
Figure 5.5(b)	$v_2 = 0.75$	134
Figure 5.5(c)	$v_2 = 1$	134
Figure 5.5(d)	$v_2 = 1.5$	134
Figure 5.6	Two adjacent cubic fractional Bézier-like curves with F^0 continuity.	139
Figure 5.6(a)	$v_1 = 0.5$ and $v_2 = 0$	139
Figure 5.6(b)	$v_1 = 0.5$ and $v_2 = 0.35$	139
Figure 5.6(c)	$v_1 = 1$ and $v_2 = 0.35$	139
Figure 5.6(d)	$v_1 = 1.5$ and $v_2 = 1$	139
Figure 5.7	Two adjacent cubic fractional Bézier-like curves with F^1 continuity.	140
Figure 5.7(a)	$v_1 = 0.5$ and $v_2 = 0$	140
Figure 5.7(b)	$v_1 = 0.5$ and $v_2 = 0.35$	140
Figure 5.7(c)	$v_1 = 1$ and $v_2 = 0.35$	140
Figure 5.7(d)	$v_1 = 1.5$ and $v_2 = 1$	140
Figure 5.8	Two adjacent cubic fractional Bézier-like curves with F^2 continuity.	142
Figure 5.8(a)	$v_1 = 0$	142
Figure 5.8(b)	$v_1 = 0.5$	142
Figure 5.8(c)	$v_1 = 0.75$	142
Figure 5.8(d)	$v_1 = 1$	142
Figure 5.9	Fractional parameter v_2 controls the curve adjustability of $f_2(t)$ for F^2 continuity between two curves.	143
Figure 5.9(a)	$v_2 = 0.5$	143

Figure 5.9(b)	$v_2 = 0.75$.	143
Figure 5.9(c)	$v_2 = 1$.	143
Figure 5.9(d)	$v_2 = 1.25$.	143
Figure 5.10	F^2 continuity of three consecutive cubic fractional Bézier-like curves.	146
Figure 5.10(a)	$v_1 = v_2 = v_3 = 0$.	146
Figure 5.10(b)	$v_1 = 0.5$ and $v_2 = v_3 = 0$.	146
Figure 5.10	(Continue) F^2 continuity of three consecutive cubic fractional Bézier-like curves.	147
Figure 5.10(c)	$v_2 = 0.25$ and $v_1 = v_3 = 0$.	147
Figure 5.10(d)	$v_1 = 0.5$, $v_2 = 0.25$ and $v_3 = 0$.	147
Figure 5.10(e)	$v_1 = v_2 = 0.5$ and $v_3 = 0$.	147
Figure 5.10(f)	$v_1 = 1$, $v_2 = 0.5$ and $v_3 = 0$.	147
Figure 5.11	Fractional parameter v_3 controls the curve adjustability of $f_3(t)$ for F^2 continuity between three curves.	148
Figure 5.11(g)	$v_1 = 1$, $v_2 = 0.5$ and $v_3 = 0.5$.	148
Figure 5.11(h)	$v_1 = 1$, $v_2 = 0.5$ and $v_3 = 0.75$.	148
Figure 5.11(i)	$v_1 = 1$, $v_2 = 0.5$ and $v_3 = 1$.	148
Figure 5.12	Examples of two parametric curves connected with degree of zero, one and two continuity, respectively.	151
Figure 5.12(a)	Degree of zero continuity.	151
Figure 5.12(b)	Degree of one continuity.	151
Figure 5.12	(Continue) Examples of two parametric curves connected with degree of zero, one and two continuity, respectively.	152
Figure 5.12(c)	Degree of two continuity.	152
Figure 5.13	Curvature plot and comb of C^0 continuity with variation of v_2	155

Figure 5.13(d) $v_2 = 0$	155
Figure 5.13(e) $v_2 = 0.5$	155
Figure 5.13(f) $v_2 = 0.75$	155
Figure 5.14 Curvature plot and comb of C^1 continuity with variation of v_2	156
Figure 5.14(a) $v_2 = 0$	156
Figure 5.14(b) $v_2 = 0.5$	156
Figure 5.14(c) $v_2 = 0.75$	156
Figure 5.15 Curvature plot and comb of C^2 continuity with variation of v_2	156
Figure 5.15(a) $v_2 = 0$	156
Figure 5.15(b) $v_2 = 0.5$	156
Figure 5.15(c) $v_2 = 0.75$	156
Figure 5.16 Curvature plot and comb of G^1 continuity with variation of v_2	157
Figure 5.16(a) $v_2 = 0$	157
Figure 5.16(b) $v_2 = 0.5$	157
Figure 5.16(c) $v_2 = 0.75$	157
Figure 5.17 Curvature plot and comb of G^2 continuity with variation of v_2	158
Figure 5.17(a) $v_2 = 0$	158
Figure 5.17(b) $v_2 = 0.5$	158
Figure 5.17(c) $v_2 = 0.75$	158
Figure 5.18 Curvature plot and comb of F^0 continuity with variation of v_1 and v_2	159
Figure 5.18(a) $v_1 = 0.5$ and $v_2 = 0$	159

Figure 5.18(b)	$v_1 = v_2 = 0.5$	159
Figure 5.18(c)	$v_1 = v_2 = 0.75$	159
Figure 5.19	Curvature plot and comb of F^1 continuity with variation of v_1 and v_2	160
Figure 5.19(a)	$v_1 = 0.5$ and $v_2 = 0$	160
Figure 5.19(b)	$v_1 = v_2 = 0.5$	160
Figure 5.19(c)	$v_1 = v_2 = 0.75$	160
Figure 5.20	Curvature plot and comb of F^2 continuity with variation of v_1 and v_2	160
Figure 5.20(a)	$v_1 = 0.5$ and $v_2 = 0$	160
Figure 5.20(b)	$v_1 = v_2 = 0.5$	160
Figure 5.20(c)	$v_1 = v_2 = 0.75$	160
Figure 6.1	Two biquartic fractional Bézier-like surfaces connected by F^0 continuity with variation of fractional parameters.	183
Figure 6.1(a)	$v_{1,1} = v_{1,2} = v_{2,1} = v_{2,2} = 0$	183
Figure 6.1(b)	$v_{1,1} = v_{2,1} = 0$, $v_{1,2} = 0.5$ and $v_{2,2} = 0$	183
Figure 6.1(c)	$v_{1,1} = v_{2,1} = 0$, $v_{1,2} = 0.5$ and $v_{2,2} = 0.5$	183
Figure 6.1(d)	$v_{1,1} = v_{2,1} = 0$, $v_{1,2} = 0.75$ and $v_{2,2} = 0.5$	183
Figure 6.1(e)	$v_{1,1} = v_{2,1} = v_{2,2} = 0.5$ and $v_{1,2} = 0.75$	183
Figure 6.1(f)	$v_{1,1} = v_{2,1} = v_{1,2} = 0.75$ and $v_{2,2} = 0.5$	183
Figure 6.2	Two biquartic fractional Bézier-like surfaces connected by F^1 continuity with variation of fractional parameters.	184
Figure 6.2(a)	$v_{1,1} = v_{1,2} = v_{2,1} = v_{2,2} = 0$	184
Figure 6.2(b)	$v_{1,1} = v_{2,1} = v_{2,2} = 0$ and $v_{1,2} = 0.5$	184
Figure 6.2(c)	$v_{1,1} = v_{2,1} = 0$, $v_{1,2} = 0.5$ and $v_{2,2} = 0.5$	184

Figure 6.2(d)	$v_{1,1} = v_{2,1} = 0, v_{1,2} = 0.75$ and $v_{2,2} = 0.5$	184
Figure 6.2(e)	$v_{1,1} = v_{2,1} = v_{2,2} = 0.5$ and $v_{1,2} = 0.75$	184
Figure 6.2(f)	$v_{1,1} = v_{2,1} = v_{1,2} = 0.75$ and $v_{2,2} = 0.5$	184
Figure 6.3	Two biquartic fractional Bézier-like surfaces connected by F^2 continuity with variation of fractional parameters.	185
Figure 6.3(a)	$v_{1,1} = v_{1,2} = v_{2,1} = v_{2,2} = 0$	185
Figure 6.3(b)	$v_{1,1} = v_{2,1} = 0, v_{1,2} = 0.5$ and $v_{2,2} = 0$	185
Figure 6.3(c)	$v_{1,1} = v_{2,1} = 0, v_{1,2} = 0.5$ and $v_{2,2} = 0.5$	185
Figure 6.3(d)	$v_{1,1} = v_{2,1} = 0, v_{1,2} = 0.75$ and $v_{2,2} = 0.5$	185
Figure 6.3(e)	$v_{1,1} = v_{2,1} = v_{2,2} = 0.5$ and $v_{1,2} = 0.75$	185
Figure 6.3(f)	$v_{1,1} = v_{2,1} = v_{1,2} = 0.75$ and $v_{2,2} = 0.5$	185
Figure 6.4	Variation of shape parameters of two biquartic fractional Bézier-like surfaces with F^2 continuity.	187
Figure 6.4(a)	First variation of shape parameters.	187
Figure 6.4(b)	Second variation of shape parameters.	187
Figure 6.4(c)	Third variation of shape parameters.	187
Figure 6.4(d)	Fourth variation of shape parameters.	187
Figure 6.5	Variation of scale factor of two biquartic fractional Bézier-like surfaces with F^2 continuity.	188
Figure 6.5(a)	$\phi = 1$	188
Figure 6.5(b)	$\phi = 0.9$	188
Figure 6.5(c)	$\phi = 1.5$	188
Figure 6.5(d)	$\phi = 2$	188
Figure 6.6	Three consecutive biquartic fractional Bézier-like surfaces formed the Möbius strip and connected by F^2 continuity with variation of fractional parameters.	189

Figure 6.6(a)	$v_{1,2} = v_{2,2} = 0$.	189
Figure 6.6(b)	$v_{1,2} = 0.5$ and $v_{2,2} = 0$.	189
Figure 6.6	(Continue) Three consecutive biquartic fractional Bézier-like surfaces formed the Möbius strip and connected by F^2 continuity with variation of fractional parameters.	190
Figure 6.6(c)	$v_{1,2} = 0.5$ and $v_{2,2} = 0.6$.	190
Figure 6.6(d)	$v_{1,2} = 0.8$ and $v_{2,2} = 0.6$.	190
Figure 6.6(e)	$v_{1,2} = v_{2,2} = 0.8$.	190
Figure 6.6(f)	$v_{1,2} = v_{2,2} = 1$.	190
Figure 6.7	Two consecutive fractional Bézier-like surfaces with Gaussian and mean curvatures masking and color coding bar with variation of shape parameters.	191
Figure 6.7(a)	Gaussian: Shape parameters are the same as Figure 6.4(b).	191
Figure 6.7(b)	Mean: Shape parameters are the same as Figure 6.4(b).	191
Figure 6.7(c)	Gaussian: Shape parameters are the same as Figure 6.4(c).	191
Figure 6.7(d)	Mean: Shape parameters are same the as Figure 6.4(c).	191
Figure 6.8	Two consecutive fractional Bézier-like surfaces with Gaussian and mean curvatures masking and color coding bar with variation of fractional parameters.	193
Figure 6.8(a)	Gaussian: $v_{1,1} = v_{1,2} = v_{2,1} = v_{2,2} = 0$.	193
Figure 6.8(b)	Mean: $v_{1,1} = v_{1,2} = v_{2,1} = v_{2,2} = 0$.	193
Figure 6.8(c)	Gaussian: $v_{1,1} = v_{2,1} = 0$, $v_{1,2} = 0.5$ and $v_{2,2} = 0$.	193
Figure 6.8(d)	Mean: $v_{1,1} = v_{2,1} = 0$, $v_{1,2} = 0.5$ and $v_{2,2} = 0$.	193
Figure 6.8(e)	Gaussian: $v_{1,1} = v_{2,1} = 0$, $v_{1,2} = 0.75$ and $v_{2,2} = 0$.	193
Figure 6.8(f)	Mean: $v_{1,1} = v_{2,1} = 0$, $v_{1,2} = 0.75$ and $v_{2,2} = 0$.	193

Figure 6.9	The closed up visualization of surfaces with F^2 continuity at194 the boundary line.
Figure 7.1	The process of "cut and combine" technique200
Figure 7.1(a)	First step.200
Figure 7.1(b)	Second step.200
Figure 7.1(c)	Third step.200
Figure 7.1(d)	Fourth step.200
Figure 7.2	The process of fitting curves involves use of piecewise clas-201 sical Bézier curves with multiple degrees (quadratic, cubic and quartic).
Figure 7.2(a)	Image of a leaf.201
Figure 7.2(b)	Curve fitting process.....201
Figure 7.2(c)	Curvature comb of Figure 7.2b.201
Figure 7.2(d)	Curve fitting process without original picture.201
Figure 7.3	Curve fitting of a leaf with F^0 continuity.....204
Figure 7.3(a)	The original outline shape without any modifications.204
Figure 7.3(b)	Curvature comb of (a).204
Figure 7.3(c)	Fractional parameters of F^0 joints are adjusted.204
Figure 7.3(d)	Curvature comb of (c).204
Figure 7.3(e)	Shape parameters of subsequent curves are adjusted.204
Figure 7.3(f)	Curvature comb of (e).204
Figure 7.4	Curve fitting of a leaf with F^1 continuity.....205
Figure 7.4(a)	The original outline shape without any modifications.205
Figure 7.4(b)	Curvature comb of (a).205
Figure 7.4(c)	Fractional parameters of F^1 joints are adjusted.205
Figure 7.4(d)	Curvature comb of (c).205

Figure 7.4(e)	Shape parameters of subsequent curves are adjusted.	205
Figure 7.4(f)	Curvature comb of (e).	205
Figure 7.5	Curve fitting of a leaf with F^2 continuity.	206
Figure 7.5(a)	The original outline shape without any modifications.	206
Figure 7.5(b)	Curvature comb of (a).	206
Figure 7.5(c)	Fractional parameters of F^2 joints are adjusted.	206
Figure 7.5(d)	Curvature comb of (c).	206
Figure 7.5(e)	Shape parameters of subsequent curves are adjusted.	206
Figure 7.5(f)	Curvature comb of (e).	206
Figure 7.6	Curve fitting process without original picture for F^0 , F^1 and F^2 continuities.	207
Figure 7.6(a)	F^0 continuity.	207
Figure 7.6(b)	F^1 continuity.	207
Figure 7.6(c)	F^2 continuity.	207
Figure 7.7	Pikachu head image. (Source: https://www.pinterest.pt/pin/318207529927050146/)	208
Figure 7.8	Curve fitting process of Pikachu using F^0 continuity.	209
Figure 7.8(a)	The original outline shape without any modifications.	209
Figure 7.8(b)	Fractional and shape parameters are adjusted.	209
Figure 7.8(c)	Curve fitting process without original image.	209
Figure 7.9	Curve fitting process of Pikachu using F^1 continuity.	210
Figure 7.9(a)	The original outline shape without any modifications.	210
Figure 7.9(b)	Fractional and shape parameters are adjusted.	210
Figure 7.9(c)	Curve fitting process without original image.	210

Figure 7.10	Formation of local curvature maximum at the endpoint using214	Corollary 7.1.1.
Figure 7.10(a)	$v_1 = 0$214	
Figure 7.10(b)	$v_1 = 0.8$214	
Figure 7.10(c)	$v_1 = 1$214	
Figure 7.11	Two piecewise κ -curves construction using two quadratic216	fractional Bézier-like curves via Algorithm 7.1.
Figure 7.11(a)	$v_1 = 0$216	
Figure 7.11(b)	$v_1 = v_{max} = 0.75$216	
Figure 7.12	Three piecewise κ curves construction using three fractional219	Bézier-like curves via Algorithm 7.2.
Figure 7.12(a)	The first curve is quintic fractional Bézier-like curve.219	
Figure 7.12(b)	The second curve is connected using G^2 continuity.219	
Figure 7.12(c)	The fractional parameter v_{max} is used for the second curve.219	
Figure 7.12(d)	The third curve/last curve is connected with F^2 continuity.219	
Figure 7.13	Simple closed curve modelled using Algorithm 7.2.220	
Figure 7.13(a)	All shape parameters are zero.220	
Figure 7.13(b)	Variation shape parameters 1.220	
Figure 7.13(c)	Variation shape parameters 2.220	
Figure 7.14	Complex closed curve modelled using Algorithm 7.2.221	
Figure 7.14(a)	All shape parameters are zero.221	
Figure 7.14(b)	Variation shape parameters 1.221	
Figure 7.14(c)	Variation shape parameters 2.221	
Figure 7.15	Bird shape modelled using Algorithm 7.2222	
Figure 7.15(a)	All shape parameters are zero.222	
Figure 7.15(b)	First variation shape parameters.222	

Figure 7.15(c) Second variation shape parameters.	222
Figure 7.16 Ruled surface constructed from two cubic fractional Bézier- like curves with various shape parameters.	228
Figure 7.16(a) $(0, 0, 0, 0, 0, 0)$	228
Figure 7.16(b) $(0.5, -1.5, 1, -2, 0.5, 1)$	228
Figure 7.16(c) $(-2.5, 1.25, -0.8, -2.5, -1.5, 1)$	228
Figure 7.16(d) $(-0.8, -1, 2, 1, -1, 2)$	228
Figure 7.17 Ruled surface constructed from two cubic fractional Bézier- like curves with various fractional parameters.	229
Figure 7.17(a) $v_1 = 0.5$ and $v_2 = 0$	229
Figure 7.17(b) $v_1 = 0.5$ and $v_2 = 0.5$	229
Figure 7.17(c) $v_1 = 0.75$ and $v_2 = 1$	229
Figure 7.18 Ruled surface constructed from the same two cubic frac- tional Bézier-like curves as in Figure 7.16(c) but with var- ious fractional parameters.	229
Figure 7.18(a) $v_1 = 0.5$ and $v_2 = 0$	229
Figure 7.18(b) $v_1 = 0.5$ and $v_2 = 0.5$	229
Figure 7.18(c) $v_1 = 0.75$ and $v_2 = 1$	229
Figure 7.19 Two fractional Bézier-like ruled surfaces connected with F^2	232
Figure 7.19(a) $w_{1,1} = w_{1,2} = w_{2,1} = w_{2,2} = 0$	232
Figure 7.19(b) $w_{1,1} = 0.5$ and $w_{1,2} = w_{2,2} = w_{2,2} = 0$	232
Figure 7.19(c) $w_{1,1} = 0.5$, $w_{1,2} = 0.75$ and $w_{2,2} = w_{2,2} = 0$	232
Figure 7.19(d) $w_{1,1} = 0.5$, $w_{1,2} = 0.75$, $w_{2,2} = 0.6$ and $w_{2,2} = 0$.	232
Figure 7.19(e) $w_{1,1} = 0.5$, $w_{1,2} = 0.75$, $w_{2,2} = 0.6$ and $w_{2,2} = 1$.	232
Figure 7.19(f) $w_{1,1} = 0.6$, $w_{1,2} = 0.8$, $w_{2,2} = 0.7$ and $w_{2,2} = 1.25$	232

Figure 7.20	Quintic fractional Bézier-like curves formed the swept sur- faces with the multiple values of shape parameters but $v_1 =$ $v_2 = 0$.	236
Figure 7.20(a)	$(0, 0, 0, 0, 0)$.	236
Figure 7.20(b)	$(-4, -3, 0.5, -3, -4, -3, -2, -0.5, -2, 3)$.	236
Figure 7.20(c)	$(3, 2.5, -0.5, 2.5, 2, 3, 1, 1, 2, 4)$.	236
Figure 7.20(d)	$(-4.9, -3.9, 3, 3.9, 4.9,$ $-4.9, -3.9, -2, 3.9, 4.9)$.	236
Figure 7.21	Quintic fractional Bézier-like curves formed the swept sur- face with variation of v_1 .	237
Figure 7.21(a)	$v_1 = 0.5$ and $v_2 = 0$.	237
Figure 7.21(b)	$v_1 = 0.75$ and $v_2 = 0$.	237
Figure 7.21(c)	$v_1 = 1$ and $v_2 = 0$.	237
Figure 7.22	Quintic fractional Bézier-like curves formed the swept sur- face with variation of v_2 .	237
Figure 7.22(a)	$v_1 = 0$ and $v_2 = 0.5$.	237
Figure 7.22(b)	$v_1 = 0$ and $v_2 = 0.75$.	237
Figure 7.22(c)	$v_1 = 0$ and $v_2 = 1$.	237
Figure 7.23	Swung surface from cubic fractional Bézier-like curves with the variation of scaling factor.	241
Figure 7.23(a)	$\mu = 0.25$.	241
Figure 7.23(b)	$\mu = 0.5$.	241
Figure 7.23(c)	$\mu = 0.75$.	241
Figure 7.23(d)	$\mu = 1$.	241
Figure 7.24	Swung surface from cubic fractional Bézier-like curves with different values of shape parameters	242
Figure 7.24(a)	$(0, 0, 0, 0, 0, 0)$.	242
Figure 7.24(b)	$(-2.9, 0, -0.9, -2.9, 0, -0.9)$.	242

Figure 7.24(c)	$(2.9, 0, -2.9, 2.9, 0, -2.9)$	242
Figure 7.24(d)	$(0.8, -1.2, 2.5, -0.8, 1.8, 2.2)$	242
Figure 7.25	Swung surface from cubic fractional Bézier-like curves with..... variation of v_1 and v_2	243
Figure 7.25(a)	$v_1 = 0.5$ and $v_2 = 0$	243
Figure 7.25(b)	$v_1 = 0.5$ and $v_2 = 0.5$	243
Figure 7.25(c)	$v_1 = 0.75$ and $v_2 = 0.6$	243
Figure 7.26	Rotation surface derived from cubic fractional Bézier-like curve with $v_1 = 0$ and variation of shape parameters.	245
Figure 7.26(a)	$(0, 0, 0)$	245
Figure 7.26(b)	$(0.9, 1.9, -0.9)$	245
Figure 7.26(c)	$(2.9, -1.9, -2.9)$	245
Figure 7.26(d)	$(0.8, 1.9, 2.8)$	245
Figure 7.27	Rotation surface derived from cubic fractional Bézier-like curve with numerous values of v_1 .	246
Figure 7.27(a)	$v_1 = 0.5$	246
Figure 7.27(b)	$v_1 = 0.75$	246
Figure 7.27(c)	$v_1 = 1.25$	246
Figure 7.28	Rotation surface derived from cubic fractional Bézier-like curve with numerous values of v_1 .	246
Figure 7.28(a)	$v_1 = 0.5$	246
Figure 7.28(b)	$v_1 = 0.75$	246
Figure 7.28(c)	$v_1 = 1$	246
Figure 7.29	Modeling of the vase with various shape parameters and fractional parameters.	247
Figure 7.29(a)	Original rotation surface $v_1 = 0$	247
Figure 7.29(b)	Shape change rotation surface $v_1 = 0$	247

Figure 7.29(c) Original rotation surface $\nu_1 = 0.25$	247
Figure 7.29(d) Shape change rotation surface $\nu_1 = 0.25$	247
Figure 7.29(e) Original rotation surface $\nu_1 = 0.5$	247
Figure 7.29(f) Shape change rotation surface $\nu_1 = 0.5$	247

LIST OF ALGORITHMS

		Page
Algorithm 3.1	Fractional De Casteljau Algorithm for Curve.....	61
Algorithm 4.1	Fractional de Casteljau Algorithm for Surface.....	88
Algorithm 7.1	Algorithm for Opened κ -Curve	215
Algorithm 7.2	Algorithm for Closed κ -Curve	218

LIST OF ABBREVIATIONS

CAD	Computer Aided Design
CAGD	Computer Aided Geometric Design
CAM	Computer Aided Manufacturing
FDE	Fractional Differential Equation
GHT	General Hybrid Trigonometric
LAC	Log-Aesthetic Curves
NURBS	Non-Uniform Rational B-Spline
RQT	Rational Quadratic Trigonometric
USM	Universiti Sains Malaysia

LIST OF SYMBOLS

P_i	control point of P for curve
$P_{i,j}$	control point of P for surface
Q_i	control point of Q for curve
$Q_{i,j}$	control point of Q for surface
$\kappa(t)$	curvature
$C(t)$	curvature comb
E	energy
F^r	fractional continuity of order r
v_i	fractional parameter for curve and surface
t	free parameter
$\Gamma(v)$	gamma function of order v
$\bar{B}_{i,n}(t)$	generalized fractional Bézier-like functions of n th degree
G^r	geometric continuity of order r
$N(t)$	normal vector
$f(t)$	parametric curve
C^r	parametric continuity of order r
$S(s, t)$	parametric Bézier surface with free parameter of s and t
R	radius
D_t^{-v}	Riemann-Liouville fractional integral operator with order v

d	scale factor for curvature comb
α_i	scale factor for geometric and fractional continuity for curve
ϕ	scale factor for geometric and fractional continuity for surface
a_i	shape parameter for curve
$a_{i,j}$	shape parameter for surface in s -direction
$b_{i,j}$	shape parameter for surface in t -direction
$T(t)$	tangent vector

LENGKUNG DAN PERMUKAAN BAK BÉZIER PECAHAN TERITLAK DENGAN APLIKASI

ABSTRAK

Tesis ini menggambarkan pembinaan lengkung dan permukaan Bézier estetik baru dikenali sebagai lengkung dan permukaan bak Bézier pecahan. Lengkung dan permukaan baru ini dibina menggunakan definisi pecahan kamiran Riemann-Liouville. Hasilnya, sebuah parameter baru terbentuk yang dikenali sebagai parameter pecahan. Parameter pecahan ini menambah ciri baru kepada lengkung dan permukaan iaitu ciri kebolehubahsuaian lengkung dan permukaan pecahan. Parameter pecahan ini membolehkan pengawalan panjang optimal lengkung atau permukaan tanpa menggunakan cara subbahagian untuk memotong lengkung atau permukaan tapi masih mengekalkan titik kawalan yang sama. Selain parameter pecahan, lengkung dan permukaan pecahan bak Bézier juga mempunyai parameter bentuk. Melalui parameter bentuk, lengkung atau permukaan dapat mengukuhkan keserbagunaan, membolehkan kawalan bentuk secara setempat. Tesis ini juga mempersembahkan sejenis keselantaran baru dikenali sebagai keselantaran pecahan dan mengatasi keselantaran geometri dalam beberapa aspek. Terutamanya, keselantaran pecahan membenarkan lengkung kedua atau permukaan kedua disambungkan ke mana-mana titik sepanjang lengkung pertama atau disambungkan ke mana-mana garis permukaan pertama, menawarkan lebih kelenturan dan keserbabolehan. Tambahan pula, analisis keselantaran pecahan dengan bantuan sisir kelengkungan dan plot kelengkungan untuk lengkung dan kelengkungan Gaussian dan min untuk permukaan juga diberi. Akhir sekali, lengkung dan permukaan pecahan bak Bézier juga akan diaplikasikan dalam proses pepadanan lengkung dengan kaedah "potong dan gabung", pembinaan lengkung- κ dan pembinaan permukaan kejuruteraan.

GENERALIZED FRACTIONAL BÉZIER-LIKE CURVE AND SURFACE WITH APPLICATIONS

ABSTRACT

This thesis portrays the construction of a new aesthetic Bézier curve and surface known as the generalized fractional Bézier-like curve and surface. This new curve and surface are constructed by using Riemann-Liouville fractional integral definition. As a result, a new notable parameter is created dubbed as fractional parameter. The fractional parameter added a new property to the curve and surface called fractional curve and surface adjustability. This fractional parameter enables the control of optimal length without splitting the curve or surface via subdivision method but still maintain the control points. In addition to fractional parameters, the generalized fractional Bézier-like curve and surface also encompasses shape parameters as well. By incorporating shape parameters, the curve or surface gains enhanced versatility, enabling localized control over its shape. The thesis also presents a novel concept called fractional continuity, which surpasses geometric continuity in several aspects. Notably, fractional continuity allows the second curve or second surface to seamlessly connect at any point along the first curve or connect at any line along the first surface, offering greater flexibility and versatility. In addition, the analysis of fractional continuity with the help of the curvature comb and curvature plot for the curve and Gaussian and mean curvatures for surface are also given. Last but not least, the generalized fractional Bézier-like curve and surface will be applied in curve fitting with "cut and combine" technique, construction of κ -curves and engineering surfaces construction.

CHAPTER 1

INTRODUCTION

1.1 Introduction: History of CAGD and Origin of Fractional Calculus

Computer Aided Geometric Design (CAGD) is the study of designing, computing and formulation of curves or surfaces using a computer (Boehm et al., 1994). CAGD is a unique field where it has unbreakable ties with mathematical disciplines such as approximation theory, differential geometry, algebraic geometry, functional analysis, differential equations, and numerical analysis (Boehm et al., 1994). CAGD also has a significant correlation with the computer science field.

CAGD had a long history and had been applied a long time ago before the term CAGD had been introduced. In the past, CAGD application can be observed through the ethnomathematics (study between mathematics and culture) in architecture design. As proof, it can be seen backdated to ancient times since 4000BC when Sumerians were the pioneer of the tessellation technique (Pickover, 2009). Tessellation is repetitive patterns and shapes that fit together without any gaps and overlap. Other civilizations, such as Egyptians, Persians, Romans, Greeks, Arabs, Japanese, and Chinese, also applied the tessellation technique in architecture. Each civilization has developed its own distinctive yet elementary shapes that have been employed in tessellation (Kizilörenli & Maden, 2021). However, in the Golden Age of Islam, Muslim architects took it to the next level by decorating the wall of mosques using tessellation of complex shapes. Chorbachi (1989) said that:

"If the Muslim artists, artisans, architects, builders, designers, carpenters and craftsmen knew geometry, they could not have acquired it spontaneously. They must have learned it, and therefore they must have been taught. But how were they taught? What knowledge of geometry was available for teaching? Who was teaching, and with what books or manuals? If such textbooks or manuscripts existed, then we should look for them, study their nature, clarify the problems that they resolved, distinguish what they considered as problematic in their own materials and find the geometric methods of construction they used to achieve the designs and patterns that are now recognized as artistic masterpieces."

This implies without understanding the underlying concept of geometry, it is impossible to craft such a design. The tessellation technique in the architecture design is irrefutable proof that geometry was heavily applied. In Malay civilization, ethnomathematics where geometry is applied in the designing of houses (windows, doors, and air ventilation), *songket* clothes (which is a *tenun* fabric), *mengkuang* mats (mats woven from *mengkuang* leaves), food cover (*tudung saji*) (Sulaiman & Husain, 2019). The Malay people also apply geometry in the designing of the traditional food known as *ketupat sate*. The *ketupat sate* is a steamed or boiled glutinous rice that has been wrapped using coconut leaf usually in a tessellation of diamond shape container (the shape depends on what type of *ketupat*). Eating *ketupat* has become a part of Malay culture since the Srivijaya empire era (Ramly et al., 2022). In the Renaissance Age, naval architects used drafting techniques that applied conic sections to build ships. The design techniques had been polished for centuries, bending wooden beams into optimal shapes. Fast forward to the early 20th-century era (modern era), parametric surfaces

are used as a description method in automobile manufacturing Farin (2002b).

The CAGD field becomes more popular, especially after the discovery of the Bézier method. Independently, Paul de Casteljaeu had developed the algorithm to compute the curve, but he did not publish it even though the development was a little earlier than Pierre Bézier's method. Meanwhile, Pierre Bézier derived the Bernstein polynomial to compute the curve, which is now known as the Bézier curve (Farin, 2002b). In the conference at the University of Utah in the year 1974, the CAGD field officially became its own discipline (Riesenfeld & Barnhill, 1974). Currently, CAGD has rapidly developed, specifically in representing curves and surfaces in mathematical formulations.

Bézier method is one of the famous methods to construct the free-form curve. It has simple formulation and computation with excellent geometric properties such as endpoint interpolation and convex hull. These properties make the Bézier methods a popular choice to apply in designing and manufacturing. Nevertheless, due to the limitations in controlling local shape, the B-spline method was developed as an alternative. B-spline has more advantages, especially in terms of flexibility and continuity between piecewise curves. Nevertheless, B-spline also has its own disadvantages where it has more complex definition than the Bézier method (Farin, 2002a). In the end, the choice to use which method between Bézier or B-spline depends on the situation. Sometimes, the designers used the Bézier curve, which is more practical than the B-spline when taking into consideration of simplicity of the Bézier curve. In other situations, the B-spline is preferable when considered from the continuity perspective.

On the other hand, fractional calculus extends the principles of ordinary calculus by exploring the differentiation and integration of orders that are not restricted to integer values. The historical development of fractional calculus can be traced back to an important milestone when Gottfried Wilhelm Leibniz received a letter from Guillaume de l'Hôpital. In the letter, l'Hôpital asked Leibniz, what if there is a fractional order of derivatives such as order $\frac{1}{2}$ of the simple function such as $f(x) = x$? Leibniz replied that it can be expressed by an infinite series. In the same letter, Leibniz conjectured that the half derivative of x is equal to $x\sqrt{dx}/x$. Leibniz also mentioned that the derivative would be an apparent paradox where someday, a useful consequence will be drawn (Miller & Ross, 1993).

Euler also delved into fractional calculus, further exploring its principles and applications. He wrote in 1730 that when $n \in \mathbb{Z}^+$, the ratio of $d^n p$ to dx^n can be formulated as $p(x)$. For example if $n = 2$ and $p = x^3$, then the ratio of $d^2(x^3)$ to d^2x is equal to ratio of $6x$ to 1 , that is $\frac{d^2(x^3)}{d^2x} = \frac{6x}{1}$. What type of ratio can be created if n is a fraction is the issue? If $n \in \mathbb{Z}^+$ can be discovered by further differentiation, then this makes sense. This approach does not, however, demonstrate that n is a fraction. However, it may be demonstrated with the aid of the interpolation that has been described in Euler's dissertation (Ross, 1900).

Lagrange made an indirect contribution to fractional calculus by introducing the law of indices in 1772. Although Lagrange initially stated that the law applies only to integer orders, as the theory of fractional calculus advanced, it became evident that the law holds true for arbitrary orders as well (Miller & Ross, 1993).

In 1812, Laplace introduced the fractional derivative through an integral, and in 1819, the first reference to a derivative appeared in a text. Lacroix wrote two pages out of 700 pages in his book on the topic regarding fractional derivative of arbitrary order (Lacroix, 1797). Starting from $y = x^a$ where $a \in \mathbb{Z}^+$, Lacroix developed the b th derivative as follows:

$$\frac{d^b y}{dx^b} = \frac{a!}{(a-b)!} x^{a-b}, \quad a \geq b. \quad (1.1)$$

Using Legendre's symbol which is the Gamma function, $\Gamma(a)$, it can be written as:

$$\frac{d^b y}{dx^b} = \frac{d^b}{dx^b} (x^a) = \frac{\Gamma(a+1)}{\Gamma(a-b+1)} x^{a-b}, \quad (1.2)$$

where

$$\Gamma(a) = \int_0^\infty t^{a-1} e^{-t} dt, \quad a \in \mathbb{R}^+. \quad (1.3)$$

If $a \in \mathbb{Z}^+$, then $\Gamma(a)$ can be reduced to:

$$\Gamma(a) = (a-1)!. \quad (1.4)$$

Then, when $a = 1$ and $b = 1/2$, Equation (1.2) will be reduced to

$$\frac{d^{\frac{1}{2}} y}{dx^{\frac{1}{2}}} = \frac{d^{\frac{1}{2}}}{dx^{\frac{1}{2}}} (x) = \frac{\Gamma(2)}{\Gamma(\frac{3}{2})} x^{\frac{1}{2}} = \frac{2x^{\frac{1}{2}}}{\sqrt{\pi}}. \quad (1.5)$$

Note that $\Gamma(\frac{3}{2}) = \frac{\sqrt{\pi}}{2}$. This result is fascinating since it has the same result as the modern-day Riemann-Liouville fractional derivative definition. Although the definition from Lacroix has no hint for applications of arbitrary order derivatives.

Fourier in 1882 also has developed the fractional derivatives (Ross, 1977). He

derived from the integral of $f(x)$:

$$f(x) = \frac{1}{2\pi} \int_{-\infty}^{\infty} f(\alpha) d\alpha \int_{-\infty}^{\infty} \cos(p(x-\alpha)) dp. \quad (1.6)$$

Hence, $\frac{d^n}{dx^n} \cos(p(x-\alpha)) = p^n \cos(p(x-\alpha) \frac{n\pi}{2})$ for derivative values of n . Then, Fourier generalized by replacing n with arbitrary u ,

$$\frac{d^u}{dx^u} f(x) = \frac{1}{2\pi} \int_{-\infty}^{\infty} f(\alpha) d\alpha \int_{-\infty}^{\infty} p^u \cos(p(x-\alpha) \frac{u\pi}{2}) dp. \quad (1.7)$$

Fourier mentioned that the number u would include whatever quantity, either positive or negative. The development of fractional calculus became more tremendously arisen when Niels Henrik Abel introduced fractional operations and applied fractional calculus in solving integral problems in 1823 (Ross, 1900). Abel solved the integral equation from tautochrone (isochrone problem) by using fractional calculus. The integral is as follows:

$$k = \int_0^x (x-t)^{-\frac{1}{2}} f(t) dt, \quad (1.8)$$

where k is constant. Equation (1.8) can be solved using Laplace Transformation method however, Abel used fractional calculus approach to solve the tautochrone problem. First, Abel divides both side of Equation (1.8) with $\Gamma(\frac{1}{2})$ to get following equation:

$$\frac{k}{\Gamma(\frac{1}{2})} = \frac{1}{\Gamma(\frac{1}{2})} \int_0^x (x-t)^{-\frac{1}{2}} f(t) dt. \quad (1.9)$$

Notice that the term on the right hand side of Equation (1.9) is actually half integral of

$f(x)$ and can be written as $D^{-\frac{1}{2}}(f(x))$. Hence, Equation (1.9) can be written as:

$$\frac{k}{\sqrt{\pi}} = D^{-\frac{1}{2}}(f(x)). \quad (1.10)$$

Next, Abel applied the half derivative, $D^{\frac{1}{2}}$ to solve for $f(x)$ and yield

$$f(x) = D^{\frac{1}{2}}\left(\frac{k}{\sqrt{\pi}}\right) = \frac{k}{\pi\sqrt{x}}. \quad (1.11)$$

Due to the fractional operators with suitable conditions on f , $D^{\frac{1}{2}}D^{-\frac{1}{2}}f = f$. Thus, the solution is a half derivative of a constant k ; hence $f(x)$ can be computed. This represents a crucial aspect of fractional calculus. It is important to note that the fractional derivative of a constant is not always zero, except when the constant value itself is zero.

Abel's solution is very elegant in the eyes of mathematicians. This attracts Liouville to study fractional calculus. Liouville developed his first formula of fractional derivative from the known result of derivatives with the series representation of the function (Miller & Ross, 1993). The known result of the derivatives of arbitrary order is as follows:

$$D^v e^{ax} = a^v e^{ax}. \quad (1.12)$$

Then he takes $f(x) = \sum_{n=0}^{\infty} c_n e^{a_n x}$ as a series. Then by applying Equation (1.12) with order v , he got:

$$D^v f(x) = \sum_{n=0}^{\infty} c_n a_n^v e^{a_n x}. \quad (1.13)$$

Equation (1.13) generalized a derivative order where v can be any number even a complex number. Nevertheless, a drawback of the previous definition is that it limits the

values of v to those where the series converges. To overcome this limitation, Liouville improved the definition by incorporating Euler's gamma integral, which is given by:

$$I = \int_0^{\infty} u^{a-1} e^{-xu} du, \quad a > 0, u > 0. \quad (1.14)$$

Taking $xu = t$, yields:

$$I = \int_0^{\infty} (t^{a-1} e^{-t}) \frac{dt}{x^a} = \frac{\Gamma(a)}{x^a}. \quad (1.15)$$

It also can be written as:

$$x^{-a} = \frac{1}{\Gamma(a)} I. \quad (1.16)$$

Then, he applied the fractional derivative operator D^v to both sides and substitute I from Equation (1.14):

$$D^v x^{-a} = \frac{1}{\Gamma(a)} D^v \int_0^{\infty} u^{a-1} e^{-xu} du. \quad (1.17)$$

According to Liouville's assumption, the derivatives with respect to x are regarded as arbitrary. Hence, it yields

$$D^v x^{-a} = \frac{(-1)^v}{\Gamma(a)} \int_0^{\infty} u^{a+v-1} e^{-xu} du. \quad (1.18)$$

Substituting back $xu = t$ in Equation 1.18 will yield as follows:

$$D^v x^{-a} = \frac{(-1)^v \Gamma(a+v)}{\Gamma(a)} x^{-a-v}. \quad (1.19)$$

Despite Liouville's effort, the definition was too narrow since it only can be used for a function of x^{-a} . Then several years later, G. F. Bernhard Riemann formulated frac-

tional integration theory since he was a student. Riemann thought of using the generalization of a Taylor series and formulated his first definition of fractional integral operator, $D^{-\nu}$ as follows:

$$D^{-\nu}f(x) = \frac{1}{\Gamma(\nu)} \int_c^x (x-t)^{\nu-1} f(t) dt + \Psi(x). \quad (1.20)$$

Due to the uncertainty of the lower limit c , he conjectured that it needs to be a complementary function $\Psi(x)$ to make the equation true. Note that for $\nu \geq 0$, the notation D^ν is symbolized for fractional derivative operator, while $D^{-\nu}$ is symbolized for fractional integral operator. A. Cayley mentioned that the ultimate question in Riemann's theory is the meaning of the complementary function containing infinitely arbitrary constants. This question caused considerable commotion among mathematicians. An error occurred in Liouville's evaluation of the complementary function since he did not take into account when $x = 0$. If $x = 0$, then the complementary function $\Psi(x) = 0$, however it contradicts with Liouville assumption where there exist a non-zero complementary function for all x when ν is rational. Hence, paradox occurred (Davis, 1927).

From the mentioned definition of fractional derivatives, it become the modern-day definition of fractional derivatives. In early development, the application of fractional calculus was uncommon and was more focused on the theory rather than applications. Fractional calculus, as it has progressed, has found applications in various domains of engineering and science such as diffusive transport, fluid dynamics, probability theory, and radiology (Miller & Ross, 1993). Not to mention that fractional calculus also has a close relationship with CAGD. This will become the starting point of the main motivation of this thesis.

1.2 Motivation

As mentioned earlier, it is obvious that CAGD and fractional calculus are distinct fields and emerging topics in mathematics. CAGD mainly deals with finding mathematical representation of curves and surfaces and usually applied in computer graphics, engineering design and manufacturing. Meanwhile, fractional calculus primarily solving integral and differentiation involving the non-integer order and has been applied in solving physics and engineering problems. Hence, the following question arose: Despite the differences, is there any intersection or common ground between CAGD and fractional calculus?

Addressing the question is vital because there is a possibility that there is unexplored and uncharted field waiting to be discovered from the combination of these two unique fields. Thus, the primary objective of this thesis is to investigate the correlation between CAGD and fractional calculus. This thesis want to explore the synergy between CAGD and fractional calculus especially whether the fractional order of integration or differentiation can be applied in constructing new aesthetic curves and surfaces. By finding the common ground and linking the bridge between CAGD and fractional calculus, this thesis can affirm to generate interesting new results and methods.

The study from Unser and Blu (2000) proposed interesting formulation for B-spline that caught author's attention. This study introduced the formulation for fractional B-spline using Liouville's one side power function. The fractional B-spline has unique property where it fractional order that can be applied in the approximation theory. From Unser and Blu work, the synergy of CAGD and fractional calculus can be seen where the fractional order has been embedded in the basis functions of the fractional

B-spline. According to author's research and findings, applying fractional order in the representation for construction of curves and surfaces are uncommon (see Section 2.7) for details regarding the synergy between CAGD and fractional calculus). Hence, the author's interest lies in following a similar path to Unser and Blu but with a different approach: incorporating fractional order from fractional calculus into the Bézier method.

The Bézier method is one of the most used approaches in CAGD for the curves and surfaces modelling and designing. The Bézier method's superior qualities combined with its simplicity led to its use because of its practicality. It has been used in CAGD to solve a variety of issues, including curves and surfaces construction, approximation, interpolation, and shape preservation. The standard Bézier curve, while widely used, has limitations in terms of adjusting local shape and achieving desired curve or surface lengths and sizes. These limitations can hinder precise control and customization of curves and surfaces in certain design scenarios. Therefore, creating new parametric curves and surfaces with control over shape and length is essential. The local control of shape may be accomplished by including the shape parameters in the representation. However, a different kind of parameter must be created to adjust length or size. The author wants to employ the fractional calculus idea to determine whether the concept or definition will aid in the development of the new parameter, which will serve as the thesis' primary objective.

1.3 Problem Statements

There are four problem statements that will be highlighted in this thesis. The first problem is the existing aesthetic Bézier curve and surface have a lack of curve and surface patch adjustability, especially in constructing the optimal length and size of the curves and surfaces. Next, the existing concept of continuity only permits the connection of two curves or surfaces at their endpoints or boundary lines. The continuity conditions should be generalized so that the connection between two curves or two surfaces occurs not only at their ends. In addition, the classical Bézier curve has lack control of shape especially in designing fair smooth curves and surfaces with minimal energy and smooth continuity. Last but not least, in manufacturing and design, the shape parameters in aesthetic Bézier curves and surfaces offer limited control when it comes to optimizing shape and size.

1.4 Objectives

This thesis focuses on the construction of novel aesthetic Bézier representation known as generalized fractional Bézier-like representation, which incorporate shape parameters. These new aesthetic representation will be used in construction of curves and surfaces. The research objectives of this thesis include:

1. To introduce the generalized fractional Bézier-like curve and surface with a new type of parameter called as fractional parameters to control the optimal length and size of curves and surfaces without depending on subdivision method.
2. To propose a new type of continuity called fractional continuity that allows two curves or surfaces to be connected at an arbitrary point/line of the first curve/-

surface without using subdivision method.

3. To analyze the design and fairness of the generalized fractional Bézier-like curves and surfaces via the shape and fractional parameters in aspect of continuity and minimizing energy with the help of curvature concept.
4. To apply fractional parameters of the generalized fractional Bézier-like representation in the curve fitting process, construction of κ -curves and modelling of engineering surfaces.

1.5 Scope and Limitations

There is a few scope and limitations that will be discussed in this thesis. The first scope is this research is focused on the new representation that are created from the definitions and concepts of fractional calculus. The new representation will be applied to CAGD applications without modifying the definitions of fractional calculus. Furthermore, for the purpose of this research, the new representation with the new type of parameter will be applied in the CAGD problems to utilize in the curve fitting process, construction of κ -curves and modelling of engineering surfaces.

1.6 Outline of Thesis

The thesis comprises the following chapters:

Chapter 2 covers about the background and literature review of this study. The review includes the discussion about the parametric curves and surfaces, especially the classical and some of the aesthetic Bézier curves and surfaces. In this chapter, the fairness metric of the smooth curve and surface such as continuity, and internal energy are

discussed with the help of the curvature plot and curvature comb. Moreover, the concept and definition of curve fitting is also explained. The definitions and constructions of the κ -curve and the engineering surfaces are also demonstrated in the same chapter. Furthermore, the concise history of fractional calculus will be discussed. The synergy between CAGD and fractional calculus will also be explained.

In Chapter 3, the new aesthetic Bézier representation, dubbed the generalized fractional Bézier-like representation, are introduced along with their properties. In this chapter, the new aesthetic representation will be focused on the construction of the curve. The geometric effect of the shape and fractional parameters of the generalized fractional Bézier-like curve will be analyzed. The new fractional de Casteljau Algorithm for curve construction is also explained. The smooth construction of the curve is also discussed by using the concept of internal energy.

Chapter 4 focuses on the generalized fractional Bézier-like surface. This chapter will discuss the properties of the generalized fractional Bézier-like surface and the geometric effect of the shape and fractional parameters on the surface. The fractional de Casteljau algorithm for surface construction also will be derived. Some examples of simple surfaces using the generalized fractional Bézier-like surface will be presented in this chapter. The role of shape and fractional parameters in surface analysis will be demonstrated via Gaussian and mean curvatures. Furthermore, the smooth and fair construction of surface are also analyzed via the internal energy such as stretch and bending energies.

In Chapter 5, the continuity concept of connecting two consecutive curves is dis-

cussed meticulously, especially the new continuity concept called fractional continuity. The behavior of the fractional continuity will be further analyzed with the help of the curvature plot and curvature comb in curves.

Chapter 6 divulges into the continuity conditions of fractional continuity for connecting two consecutive surfaces up until degree two. Furthermore, the behaviour of the fractional continuity in surfaces also will be discussed by using the Gaussian and mean curvatures.

Chapter 7 deals with the applications of the generalized fractional Bézier-like curve and surface. The applications such as the curve fitting process, construction of the κ -curve, and the modelling of the engineering surfaces.

Last but not least, the overall conclusion with some suggestions for future research will be presented in Chapter 8.

CHAPTER 2

BACKGROUND AND LITERATURE REVIEW

2.1 Parametric Curves and Surfaces

To generate the shape, the free-form curves and surfaces are usually become the main component due to their flexibility and practicality. To represent these free-form shapes, parametric equations are used to represent all types of curves and surfaces. Parametric curves and surfaces are particularly useful when the curves or surfaces cannot be easily expressed as functions on the Cartesian plane. This is due to the complicated Cartesian equations especially in representing curves or surfaces that have self-intersection. Moreover, if the curves or surfaces fail the Vertical Line Test (a test to show that a curve is either a function or not) then representing the shapes in Cartesian equation is impractical. Hence, by parameterization, it allows for easier representation of complex curves and surfaces (Stewart et al., 2020). This flexibility makes parametric representation a valuable tool in CAGD and other fields where complex curves or surfaces need to be modeled and analyzed. Thus, parametric equations are crucial in CAGD especially when dealing with conic sections (Metsker, 2002).

Hence, researchers create various methods and techniques to develop a good representation of the free-form parametric curves and surfaces that can be used in various conditions and situations. In CAGD, the parametric representation of curves and surfaces plays a crucial role in various industries such as architecture, shipbuilding, and manufacturing. One of the methods known as the Bézier method and this method become one of the popular tools that have been used in designing curves and surfaces.

2.1.1 Bézier Curves and Surfaces

In CAGD, the Bézier tool is widely regarded as one of the most practical tools for modeling curves and surfaces, primarily due to its remarkable geometric properties (Farin, 2002a; Prautzsch et al., 2002). The classical Bézier curve, which employs Bernstein polynomials as its basis functions, serves as a fundamental for the development of intricate curves and surfaces. Bézier curves has been developed by Pierre Bézier where in modelling a basic curve based on the intersection of two elliptical cylinders. Then, the formulation from the two elliptical cylinders are expanded to polynomial functions with higher degree.

His work caught the attention of A.R Forrest. Forrest able to represent the Bézier curves in terms of Bernstein polynomial. This implied that Bézier curves will have properties such as partition of unity, non-negativity, symmetry, linear independence, convex hull, endpoint interpolation and tangent (Farin, 2002a). The classical Bézier curve with n th degree can be defined as follows:

$$f(t) = \sum_{i=0}^n \binom{n}{i} (1-t)^{n-i} t^i P_i, \quad t \in [0, 1], \quad (2.1)$$

where P_i is the control point and $\binom{n}{i} (1-t)^{n-i} t^i$ is known as the Bernstein basis function of n th degree. Figure 2.1 shows the classical cubic Bézier curves with different set of control points.

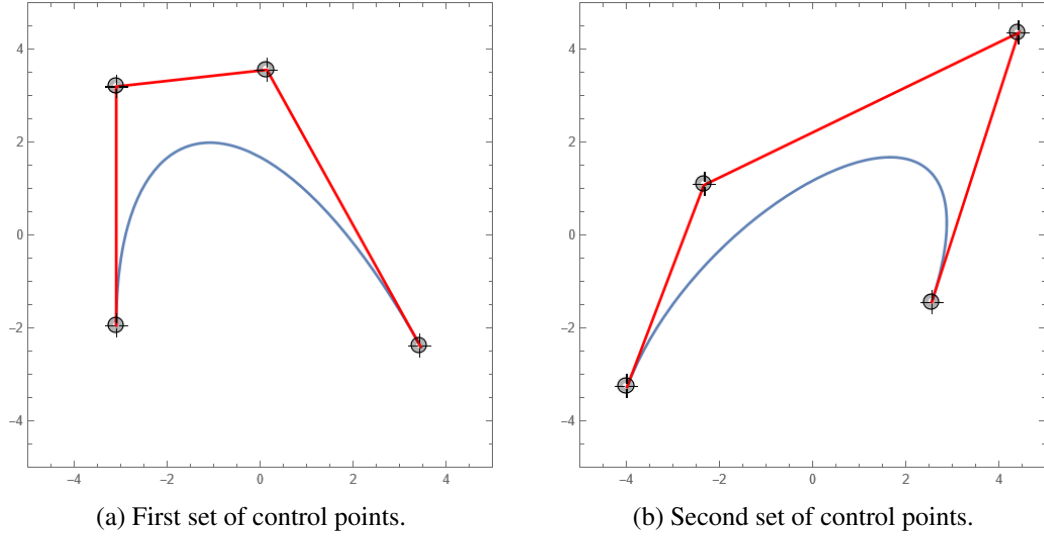


Figure 2.1: Classical cubic Bézier curves with different set of control points.

The main problem with Bézier method is the lack of local shape control. Hence, the rational Bézier curves and surfaces were developed as an upgraded version of the classical Bézier to address these restrictions. The rational Bézier curves and surfaces have weight factors that enable shapes to change without moving the control points (Mainar et al., 2001). Unlike traditional Bézier curves and surfaces, the rational Bézier curves and surfaces, defined by rational functions, introduce significantly more complex computations, challenging integrals, and recurring differentiation (Hu et al., 2018b). The traditional Bézier basis functions must be modified in order to keep the good geometric representation and characteristics of the Bézier curves while enhancing shape flexibility, approximation, and length adjustability. As a result, several academics discovered a solution by including a shape parameter into the new basis functions resulting a new creation of aesthetic Bézier curves and surfaces.

2.1.2 Aesthetic Bézier Curves and Surfaces

To achieve more control over the design of curves, it is necessary to construct basis functions by incorporating shape parameters. The local shape can be controlled by

simply varying the values of the shape parameters and still maintain the convex hull. Bézier method are highly essential in curve and surface design due to their ability to interpolate at both endpoints and capable to undergo the subdivision process. However, when a higher curve degree is used to fit or interpolate a large number of points, the current classical or aesthetic Bézier curves have higher tendency to overshoot. This is because the higher degree of curve implied higher number of control points. Having more control points provide more flexibility but makes the process of control points placement much harder since Bézier curve is sensitive to the control points locations. If the control point is poorly positioned, then the tendency to overshoot is higher especially if they is a sudden change in the shape of curve. Overshoot in CAGD is where the curve or surface constructed over-passed the constraint or control points. Hence, it is feasible to get around this problem by adjusting the curve's ideal length. In addition, the classical Bézier curve and surface can only give approximation representation of conic sections. From the mentioned limitations, researchers have developed the modified version of the classical Bézier curves and surfaces which have more malleability but still maintaining the traditional Bézier properties which known as the aesthetic Bézier curves and surfaces.

The goal of developing aesthetic Bézier method is to overcome the constraint of classical Bézier method, which states that changing the shape requires changing the control points. Therefore, in order to overcome this restriction, numerous researchers developed the aesthetically pleasing Bézier curve with shape parameters. For instance, the generalized Bézier curve with shape parameters via integral technique was introduced in Wang and Wang (2005). Yang and Zeng (2009) constructed a Bézier curve with n shape parameters of n th degree. Adding shape parameters would provide local

shape adjustment, thus, increasing flexibility.

The conic sections can also be approximated using the rational Bézier curves. Therefore, in order to provide a more precise approximation of the conic sections and also exact representation of some conic sections, researchers devised the trigonometric Bézier basis functions. Bashir et al. (2012) proposed rational quadratic trigonometric curves and it can represent the elliptic arc. Meanwhile, the cubic trigonometric Bézier-like curves derived by Usman et al. (2020) can represent the elliptic and parabolic arcs. Ammad et al. (2022) created the generalized trigonometric Bézier curve by introducing n th degree of trigonometric basis functions with two shape parameters and can give representation of circular and elliptic arcs.

The examples provided in Yan et al. (2017) and Yuksel (2020) show the use of Bézier curves to construct objects, ensuring that the resulting curves are free from self-intersections. Different levels of continuity and curves degrees can be employed to create self-intersection-free curves (Adnan et al., 2020). Next, it is a quite inconsistent to interpolate the endpoints using different Bézier curves degrees since it can disturb the uniform and consistency of the designed curves. To generate the self-intersection-free curve using the same degree of curves, a new type of parameter is required.

The aesthetic Bézier basis functions can also be extended to construct surface. For example, the shape-adjustable generalized Bézier surfaces with $n + 1$ shape parameters is developed by Hu et al. (2018b). BiBi et al. (2019) proposed the Generalized Hybrid-Trigonometric Bézier (GHT-Bézier) basis functions by incorporating exponential and trigonometric functions with three shape parameters to construct new aesthetic

surfaces. While, Ammad and Misro (2020) has construct surfaces from quintic trigonometric Bézier basis functions with two shape parameters. The hyperbolic functions are also incorporated in the aesthetic Bézier basis functions to generate surfaces called as the H-Bézier surfaces (Li et al., 2020).

In summary, the advantages of the aesthetic Bézier curves and surfaces are the local control of shape of curves and surfaces without altering the control points via shape parameters. In addition, some of the aesthetic Bézier curves and surfaces can give exact representation of conic sections. However, the glaring limitation of most of the aesthetic Bézier curves and surfaces is they do not have subdivision method in order to construct the fraction of the curves or surfaces. Only classical Bézier curves and surfaces can undergo subdivision method due to de Casteljau algorithm. Hence, it has been the aim of this thesis to construct aesthetic Bézier curves or surfaces that have shape parameters but still able to employ subdivision method or any alternative method that has same effect with the subdivision method.

2.2 Fairness Metric of Construction of Smooth Curve and Surface

Smooth curves and surfaces are essential in engineering and architecture in order to manufacture elegant products and keeping structures from collapsing, especially when working with a variety of shapes and lengths. It is possible to create smooth curves and surfaces by adhering to specific fairness rules. The measures that are frequently utilized to assess the fairness of curves and surfaces include continuity conditions, internal energy, and curvature analysis.

2.2.1 Continuity of The Curve

Curve modelling can occasionally be delayed due to the complex nature of curve design. By utilising continuity, which allows complicated curves to be divided into simpler curves, this issue may be fixed. Given their ability to allow two curves to link smoothly, parametric and geometric continuities have significantly grown in curve modelling. The parametric and geometric continuities of order r are symbolized by C^r and G^r , respectively. These two kinds of continuities are typically used as benchmarks in creating smooth curves and surfaces.

Numerous research has been done regarding continuity of parametric curves and aesthetic curves. For example, DeRose and Barsky (1985) provided a meticulous discussion on the concepts of parametric and geometric continuity in the context of parametric curves. In the work by Barsky and DeRose (1990), the establishment of geometric continuity for both the Bézier curve and the Beta spline (B-spline) was thoroughly investigated. Researchers have discussed the C^0 , C^1 , and C^2 continuity, as well as the G^0 , G^1 , and G^2 continuity, for various aesthetic Bézier curves, including the general Bézier (GE-Bézier) curve with n shape parameters (Qin et al., 2013) and the Rational Quadratic Trigonometric Bézier (RQT-Bézier) curve with two shape parameters (Bashir et al., 2012). The same level of parametric and geometric continuity was also studied for the Q-Bézier curve and the quintic trigonometric Bézier curve with two shape parameters (Hu et al., 2017a; Misro et al., 2017). General Hybrid Trigonometric Bézier (GHT-Bézier) curve, which is another aesthetic Bézier curve, also studied the parametric continuity and geometric continuity of the corresponding curves up to C^3 and G^3 in BiBi et al. (2020).

2.2.2 The Internal Energy of Curve

Another crucial element in determining smooth curves and surfaces is the internal energy. In general, maximising curve smoothness is resulted from minimization of internal energy (Horn, 1983; Wesselink & Veltkamp, 1995). The arc length and bending energy were explicitly studied in relation to the quadratic Bézier curve and its applications in Ahn et al. (2014). The geometric construction of the minimal energy for the generalized Bézier curve was first introduced by Xu et al. (2011). Next, Ahn et al. (2014) suggested a method for determining the geometric constraints on quadratic Bézier curves using the least amount of length and energy. Meanwhile, the finding of the minimal jerk energy for Bézier curves utilising related matrices was discussed in Erişkin and Yücesan (2016). In a recent study in Li and Zhang (2020), the planar cubic G^1 Hermite interpolation curves were investigated regarding the aspect of minimizing length and curvature variation energy.

The aim of curve modelling often involves creating a smooth curve. The smoothness of the curve will be maximized by reducing an appropriate amount of energy (Wesselink & Veltkamp, 1995). One of the important techniques in curve modelling is thought to be minimizing the curve's energy. The external energy, $E_{external}$ and internal energy, $E_{internal}$ that make up the total energy, E_{total} in the curve are often expressed by the following equation:

$$E_{total} = E_{external} + E_{internal}. \quad (2.2)$$

The curve's external energy is a portion of the overall energy that is dependent on factors outside of the curve, such as its surroundings. To calculate external energy,

$E_{external}$, the external forces need to be identified. As example, the external forces can be from friction, gravity and wind. The energy generated by the characteristics (such as the curve's shape) and behaviour of the curve itself is known as the internal energy of the curve. The overall shape and characteristics of the curve will be determined by this internal energy (Wesselink & Veltkamp, 1995). According to Veltkamp and Wesselink (1995), the relevant energy function typically depends on the local characteristics of the curve, such as curvature and tangent vector (i.e. internal energy). The internal energy of curve can be written as the sum of stretch energy, $E_{stretch}$, bending energy, $E_{bending}$ and curvature variation energy, E_{cv} . The equation is as follows:

$$E_{internal} = E_{stretch} + E_{bending} + E_{cv}. \quad (2.3)$$

In this thesis, the minimizing of internal energy will be the main focus. The definitions of stretch energy, $E_{stretch}$, bending energy, $E_{bending}$ and curvature variation energy, E_{cv} for curve will be discussed further in Chapter 3.

2.2.3 Curvature Analysis of Curves

Curvature is one of the important concepts in differential geometry. This is because by analyzing the curvature of a curve, the fairness and the smoothness of the curve can be determined (Farin & Sapidis, 1989). There are multiple interpretations of curvature (Goldman, 2005; Guoxiang, 2018):

1. The degree to which a curve deviate off a straight line.
2. The reciprocal of the circulating radius, that is, $\frac{1}{R}$, where R is the circulating